

# Ozonation: A Unique Route To Prepare Nickel Oxyhydroxides. Synthesis Optimization and Reaction Mechanism Study

F. Bardé,<sup>\*,†</sup> M. R. Palacín,<sup>‡</sup> B. Beaudoin,<sup>†</sup> and J.-M. Tarascon<sup>†</sup>

Laboratoire de Réactivité et Chimie des Solides (LRCS), Université de Picardie Jules Verne, 33 rue Saint Leu, Amiens, France, and Institut de Ciència de Materials de Barcelona (ICMAB-CSIC), Campus UAB, 08193 Bellaterra, Catalunya, Spain

Received August 9, 2004. Revised Manuscript Received October 20, 2004

This paper details the reacting paths involved during the oxidation of  $\alpha$ II-Ni(OH)<sub>2</sub> and  $\beta$ II-Ni(OH)<sub>2</sub> with ozone, which is compared to the oxidation process conducted in aqueous solution. The main advantage of the ozone method lies in the control of the reaction medium steps owing to the feasibility of operating in the presence or absence of alkaline cations. This enables the preparation of the pure  $\beta$ III-NiOOH phase, well-known to be difficult to obtain in aqueous media without  $\gamma$ III-NiOOH traces. The reaction mechanisms for both oxidation processes were found to be similar, and to yield the same final products, except for  $\alpha$ II-Ni(OH)<sub>2</sub>, where ozonation allowed the preparation of a new oxidized phase that was isolated and characterized by means of complementary techniques such as X-ray diffraction, chemical analysis, HRTEM, TGA, and FT-IR. A mechanism to account for the formation of this phase is proposed.

## Introduction

Many efforts have been made over the years to study the crystal chemistry of the nickel oxyhydroxide electrode (NOE)<sup>1,2</sup> to improve its capacity frequently perturbed by the existence of a “second plateau”, as well as to master its poor chargeability and self-discharge problems.<sup>3–5</sup>

As described by Bode in 1969, the NOE can involve different phases:  $\alpha$ II-Ni(OH)<sub>2</sub> and  $\beta$ II-Ni(OH)<sub>2</sub> in the reduced state and  $\beta$ III-NiOOH and  $\gamma$ III-NiOOH in the oxidized state.<sup>6</sup> While both the reduced phases are known to crystallize in the  $P\bar{3}m1$  space group within the hexagonal system, the crystal structure of the oxidized phases is ill-defined (i.e., space group unknown), but it is generally assumed that they all consist of parallel NiO<sub>2</sub> layers packed along the *c* axis. The differences in the structures of all these phases lie in the stacking of layers owing to the presence of species in the interlayer space, such as nitrates or carbonates for  $\alpha$ II-Ni(OH)<sub>2</sub> or alkaline cations for  $\gamma$ III-NiOOH. These interlayer species induce a more dilated *c* parameter as compared to the  $\beta$ II-Ni(OH)<sub>2</sub> or  $\beta$ III-NiOOH phases involved in commercial nickel batteries. For such applications, it is a common belief that the best battery performances are

obtained for  $\beta$ II-type samples having a higher content of defects and less crystallinity,<sup>7</sup> thus being more difficult to characterize.

Besides the electrochemical-synthesis route, the oxidized phases can also be obtained either through hydrolysis of A<sub>x</sub>NiO<sub>2</sub> (A = Na, K) using a soft chemistry approach<sup>8</sup> or by oxidation of Ni(OH)<sub>2</sub> in an aqueous solution containing NaClO.<sup>9,10</sup> However, in both cases, owing to the presence of alkaline ions in the reaction medium, the single  $\beta$ III-NiOOH phase is difficult to obtain, the product always being contaminated by traces of  $\gamma$ III-NiOOH containing alkaline ions. Numerous studies report the oxidation of nickel hydroxides, but only a few references deal with the dry oxidation process. In that context, we decided to reexamine the preparation of nickel-oxidized phases using the ozonation route. This technique is commonly used in water treatment, but is much less developed to oxidize solid phases. The first attempt of using ozone as an oxidant agent was performed by Besson et al.<sup>9</sup> in 1947, who tried to oxidize a nickel sulfate solution by bubbling ozonized oxygen inside it, and observed a blackening of the solution. Then, Megahed et al.<sup>11</sup> used an ozonation treatment of 72 h at 20 °C in the presence of alkaline ions to synthesize a large batch (1500 g) of stable  $\gamma$ III-NiOOH phase. Finally, Erreddad et al.<sup>12</sup> tested two oxidation routes: dry and aqueous oxidation on both  $\alpha$ II-Ni(OH)<sub>2</sub> and  $\beta$ II-Ni(OH)<sub>2</sub> nickel hydroxides using ozone produced from air. Starting with the  $\beta$ II-Ni(OH)<sub>2</sub> phase, the

\* To whom correspondence should be addressed. E-mail: fanny.barde@sc.u-picardie.fr.

<sup>†</sup> Université de Picardie Jules Verne.

<sup>‡</sup> ICMAB-CSIC.

- (1) Oliva, P.; Leonardi, J.; Laurent, J. F.; Delmas, C.; Braconnier, J. J.; Figlarz, M.; Fievet, F.; de Guibert, A. *J. Power Sources* **1982**, 8, 229–255.
- (2) Delahaye-Vidal, A.; Portemer, F.; Beaudoin, B.; Tekaiia-Elhissen, K.; Genin, P.; Figlarz, M. In *Nickel hydroxide electrodes*; Corrigan, D. A., Zimmerman, A. H., Eds.; The Electrochemical Society: Pennington, NJ, 1990; Vol. PV 90-4, pp 44–60.
- (3) Armstrong, R. D.; Briggs, G. W. D. *J. Appl. Electrochem.* **1988**, 18, 215–219.
- (4) Delmas, C.; Faure, C.; Gautier, L.; Guerlou-Demourges, L.; Rougier, A. *Philos. Trans. R. Soc. London, A* **1996**, 354, 1545–1554.
- (5) Watanabe, K. I.; Koseki, M.; Kumagai, N. *J. Power Sources* **1996**, 53, 23.
- (6) Bode, H.; Dehmelt, K.; Witte, J. Z. *Anorg. Allg. Chem.* **1969**, 1, 366.

- (7) Delmas, C.; Tessier, C. *J. Mater. Chem.* **1997**, 7, 8, 1439–1443.
- (8) Delmas, C.; Braconnier, J.-J.; Maazaz, A.; Hagenmuller, P. *Rev. Chim. Miner.* **1982**, 19, 343.
- (9) Besson, J. *Ann. Chim., 2<sup>ème</sup> Ser., Tome* **1947**, 2, 527–598.
- (10) Sac-Epée, N.; Palacin, M.-R.; Beaudoin, B.; Delahaye-Vidal, A.; Jamin, T.; Chabre, Y.; Tarascon, J.-M. *J. Electrochem. Soc.* **1996**, 144, 3896–3907.
- (11) Megahed, E. S.; Spellmann, P. J.; Tennare, L. *Proc. Symp. Battery Dev., Electrochem. Soc. Proc. Ser.* **1979**, 79-1, 259–282.
- (12) Khair, E. Thèse de doctorat d'état, Université de Picardie Jules Verne, Amiens, France, 1984.

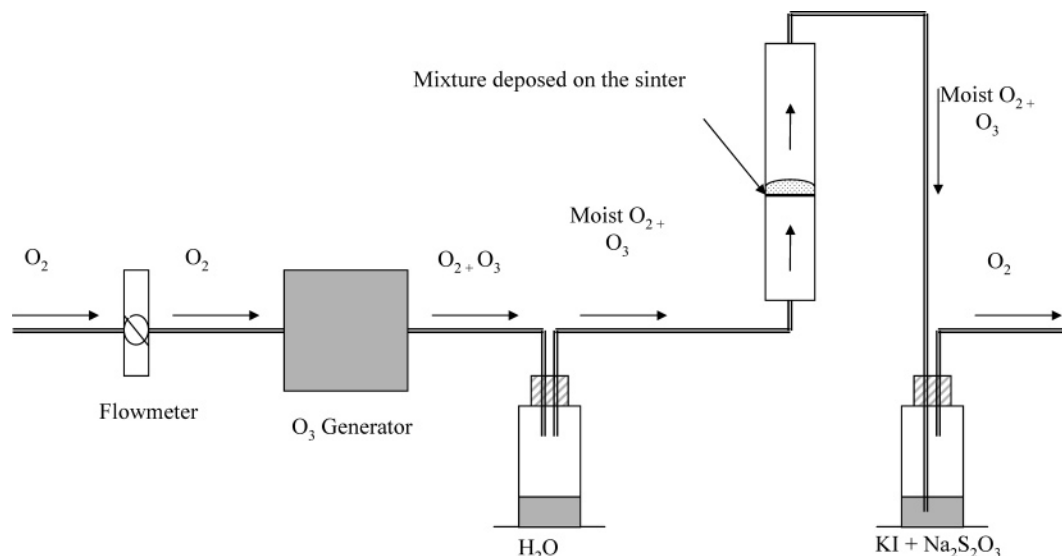


Figure 1. Scheme of the ozonation assembly.

authors obtained a mixture of  $\beta$ III-NiOOH and  $\gamma$ III-NiOOH nickel oxyhydroxides, and proposed a solid-state reaction mechanism. Starting with the  $\alpha$ II-Ni(OH)<sub>2</sub> phase, they showed a competition between the  $\alpha$ II-Ni(OH)<sub>2</sub>  $\rightarrow$   $\beta$ II-Ni(OH)<sub>2</sub> phase evolution and the direct  $\alpha$ II-Ni(OH)<sub>2</sub>  $\rightarrow$   $\gamma$ III-NiOOH oxidation reaction. More recently, our group studied the dry oxidation of cobalt hydroxide,<sup>13</sup> and showed that the ozonation is a unique route to prepare  $\gamma$ III-CoOOH oxyhydroxide besides the hydrolysis of precursors prepared at high temperature by the ceramic route. Moreover, we demonstrated that the ozonation process presents numerous benefits such as a real control of the oxidation steps, which makes possible the introduction of cations at the right moment of the reaction, and therefore enables a control of the phases obtained. Owing to the versatility of this synthesis technique, we decided, as reported herein, to study the ozonation of  $\beta$ II-Ni(OH)<sub>2</sub> and  $\alpha$ II-Ni(OH)<sub>2</sub> nickel hydroxides, following the same approach used for cobalt hydroxides.

## Experimental Section

**Syntheses of the Starting Materials.** The  $\alpha$ II-Ni(OH)<sub>2</sub> phase was obtained according to Le Bihan.<sup>14,15</sup> A 500 mL sample of a 1 molar nickel nitrate solution was added drop by drop to 65 mL of 28% ammonia solution at room temperature under strong stirring conditions. The obtained green precipitate that rapidly appeared was centrifuged, copiously washed to neutral pH, and washed a last time with acetone before being quickly dried at room temperature prior to being identified as the  $\alpha$ II phase by X-ray diffraction.

For  $\beta$ II-Ni(OH)<sub>2</sub>, a few grams of  $\alpha$ II-Ni(OH)<sub>2</sub> precursor was dispersed in water, introduced inside an autoclave, and treated at 120 °C under hydrothermal conditions.<sup>16</sup> The mixture was centrifuged and dried at 55 °C for 15 h. A green powder was obtained and identified as  $\beta$ II-Ni(OH)<sub>2</sub>.

**Ozonation System.** The experimental assembly is represented in Figure 1. The ozone is produced from a pure oxygen source

(quality 99.999%) by a BMT 803 type ozone generator, with the ozone amount formed depending on the oxygen flow that is regulated by a flow meter. Once produced, the gas crosses either a dry or a moist atmosphere, and goes into a vertical reactor containing a sinter, on top of which the sample to oxidize is placed. Typically, 1–1.5 g of powder consisting either of the hydroxide alone or a mixture of Ni(OH)<sub>2</sub> with ground KOH pellets is treated. The potassium hydroxide can be added either at the beginning or during the course of the reaction. In the latter case, we experienced that the moment of KOH addition together with its amount and the moisture content of the ozone gas are crucial in governing the degree of advancement of the reactions, and thus the synthesis of single phases. Finally, the ozone which has not been consumed through this reaction is destroyed by a reducing solution containing sodium thiosulfate and potassium iodide acting as an indicator. For safety reasons, Teflon ribbon instead of silicone paste was used in the glass connections.

**Physical Characterization.** Samples removed at different stages of the ozonation process have been investigated by X-ray diffraction, TEM, TGA, and FT-IR. Their phase composition was determined by X-ray powder diffraction using either a Phillips diffractometer, PW1729, with a Cu anticathode with  $K\alpha_1$  ( $\lambda = 1.54957\text{\AA}$ ) radiation or a Bruker D8 apparatus using a Co anticathode with  $K\alpha_{\text{moy}}$  radiation ( $\lambda = 1.79026\text{\AA}$ ). The morphology and structural changes of the samples upon oxidation were deduced from transmission electron microscopy (TEM) observations done on an STEM Phillips CM12. High-resolution transmission electron microscopy (HRTEM) was also performed using a Phillips Tecnai 200 F20 STEM microscope. Infrared spectra were collected on a 510 FT-IR Nicolet apparatus in the transmittance mode with 64 flows in the 4000/400  $\text{cm}^{-1}$  domain with a resolution of 4  $\text{cm}^{-1}$  on KBr pellets containing about 1% of the material to test. TGA measurements were performed on a Mettler Toledo apparatus, under static air with a thermal rate of 5 °C/min, in a temperature window ranging from 20 to 800 °C. The average oxidation degree of nickel in the prepared phases was determined by iodometric titration, whereas the total amount of nickel was dosed using ethylenediaminetetraacetic acid (EDTA) solution. Typically, 100 mg of the sample is added to 1.5 g of potassium iodide, and the mixture is dissolved in an acetic buffer solution. Sodium thiosulfate solution is used to titrate the iodine produced during nickel reduction. Then, 100 mL of water and 14 mL of 28% ammonia solution are added, and the complexometric titration is carried out with an EDTA solution in the

(13) Bardé, F.; Palacin, M.-R.; Beaudoin, B.; Delahaye-Vidal, A.; Tarascon, J.-M. *Chem. Mater.* **2004**, *16*, 299–306.

(14) Le Bihan, S.; Guenot, J.; Figlarz, M. *C. R. Acad. Sci.* **1970**, *270*, 2131–2133.

(15) Le Bihan, S. Thèse de doctorat d'état, Université Paris VI, Paris, 1974.

(16) Le Bihan, S.; Figlarz, M. *J. Cryst. Growth* **1972**, *13–14*, 458–435.

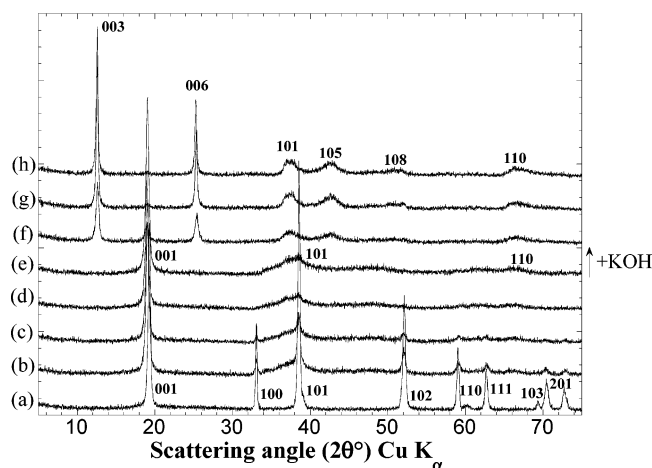


**Figure 2.** X-ray diffraction patterns of samples removed during the two-step ozonation of  $\beta$ II-Ni(OH) $_2$ : (a) initial  $\beta$ II-Ni(OH) $_2$  phase; (b) phase obtained after 30 min under a moist ozone atmosphere; (c) after 1 h; (d) after 2 h; (e) after 4 h; (f) after 5 h of moist ozone treatment with KOH addition; (g) after 6 h; (h) final product obtained after 8 h of treatment.

presence of murexide as indicator. The analyses were performed twice on each sample. The nitrate contents were determined by inductively coupled plasma mass spectrometry (ICPMS).

## Results

For reasons of clarity, the oxidation of the  $\beta$  and  $\alpha$  phases will be presented separately, and in each section we will clearly separate the two experimental protocols used, denoted protocols 1 and 2 and corresponding to the addition of the KOH at the middle or beginning of the reaction, respectively.

**Ozonation of  $\beta$ II-Ni(OH) $_2$ .** Our crystallized nickel hydroxide prepared under hydrothermal conditions presents an X-ray diffraction pattern with sharp lines (Figure 2a) reminiscent of the  $\beta$ II-Ni(OH) $_2$  having the following lattice parameters:  $a = 3.126$  Å and  $c = 4.605$  Å (in agreement with the results obtained by Greaves et al.<sup>17</sup>) and crystallizing in the hexagonal system with the  $P\bar{3}m1$  space group. The indexation of the Bragg reflections in Figure 2a was performed according to the 14-0117 JCPDS card. From a morphological point of view, this sample consists of large hexagonal platelets presenting Bragg fringes as shown in the bright field TEM images (Figure 3a). The average diameter and thickness of the particles are 1200 and 400 Å, respectively. The selected area electronic diffraction (SAED) highlights the monolithic character of the particles since very well defined spots are observed on the electron diffraction patterns (Figure 3b).

**Protocol 1.** XRD patterns of  $\beta$ II-Ni(OH) $_2$  and samples removed in the course of the reaction with ozone are represented in Figure 2. The first step of the reaction (without KOH) corresponds to the transformation of  $\beta$ II-Ni(OH) $_2$  into pure  $\beta$ III-NiOOH (denoted  $\beta$ III<sub>exβ</sub> and indexed according to the 6-0141 JCPDS file) (Figure 2e), which was found to present an oxidation degree of  $3.00 (\pm 0.05)$  as deduced from chemical titration. After 2 h of treatment, most of the  $\beta$ II-Ni(OH) $_2$  lines have disappeared (see Figure 2c). A small shift of the (001) reflection corresponding to an increase in the  $c$

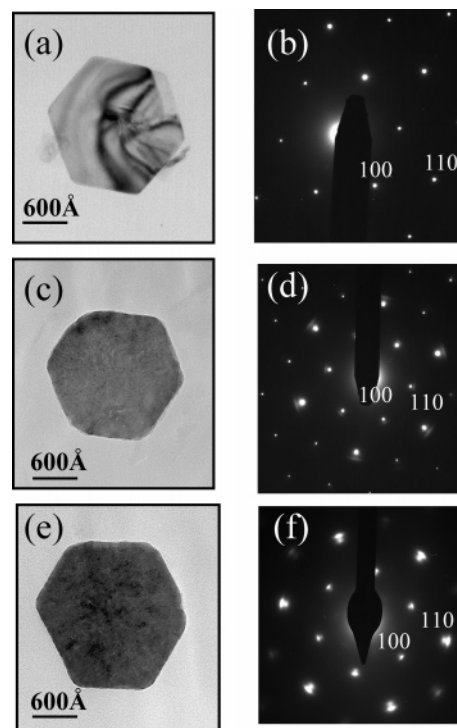


**Figure 3.** Transmission electronic microscopy images: (a) platelet of the initial  $\beta$ II-Ni(OH) $_2$  product; (b) SAED on the particle represented in (a); (c) platelet from a sample after 1 h of reaction under moist ozone without KOH; (d) SAED on the particle represented in (c); (e) platelet from a sample after 6 h of reaction under moist ozone with KOH; (f) SAED on the particle represented in (e).

cell parameter changing from 4.605 to 4.83 Å and reminiscent of the  $\beta$ II-Ni(OH) $_2 \rightarrow \beta$ III-NiOOH oxidation process is observed. This sample was also analyzed by TEM. The bright field images (Figure 3c) indicate that the size and shape of the particles are maintained upon ozonation, while important textural changes occur, with, namely, the initial monolithic  $\beta$ II-Ni(OH) $_2$  particles becoming mosaic. Moreover, the dark field images highlight the pseudomorphic character of ozonation. Indeed, the SAED (Figure 3d) on a single particle shows the coexistence of  $\beta$ II-Ni(OH) $_2$  and  $\beta$ III-NiOOH phases. A topotactic relation between the phases with  $(100)_{\beta\text{III}} // (100)_{\beta\text{II}}$  and  $(110)_{\beta\text{III}} // (110)_{\beta\text{II}}$  also exists. The reflections corresponding to  $\beta$ III are broad arcs as compared to well-defined spots for the  $\beta$ II phase. In short, TEM observations confirm the XRD results, and reveal the coexistence of both  $\beta$ II-Ni(OH) $_2$  and  $\beta$ III-NiOOH within this sample. In contrast, if ozonation is pursued in the presence of KOH (second step),  $\beta$ III-NiOOH is shown to transform into the  $\gamma$ III-NiOOH phase for which Bragg peaks have been indexed in agreement with the 6-0075 JCPDS file. According to complementary XRD and TEM results, the  $\beta$ III/ $\gamma$ III transformation was also found to be pseudomorphic and topotactic (Figure 3e,f), leading to a mosaic  $\gamma$ -type phase with an average nickel oxidation state equal to  $3.55 (\pm 0.05)$ .

**Protocol 2.** A solid mixture of  $\beta$ II-Ni(OH) $_2$  and KOH was treated under a moist ozone atmosphere. Figure 4 exhibits the X-ray diffraction patterns of several samples removed during ozone treatment. We can note, in the early stage of the reaction, the appearance of Bragg reflections characteristic of both the  $\beta$ III-NiOOH and  $\gamma$ III-NiOOH oxidized phases together with those of the initial  $\beta$ II-Ni(OH) $_2$  phase.

(17) Greaves, C.; Thomas, M. A. *Acta Crystallogr., Sect. B* **1986**, 42, 51–55.



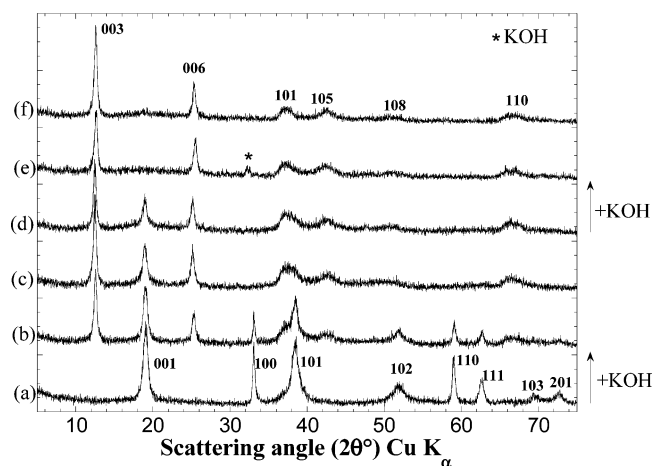


**Figure 4.** X-ray diffraction patterns of different samples taken off during the one-step ozonation of  $\beta$ II-Ni(OH)<sub>2</sub>: (a) initial  $\beta$ II-Ni(OH)<sub>2</sub> phase; (b) after 9 h of reaction under a moist ozone atmosphere in the presence of KOH; (c) after 34 h; (d) after 126 h; (e) after 135 h and another KOH addition; (f) final product obtained after 148 h of treatment.

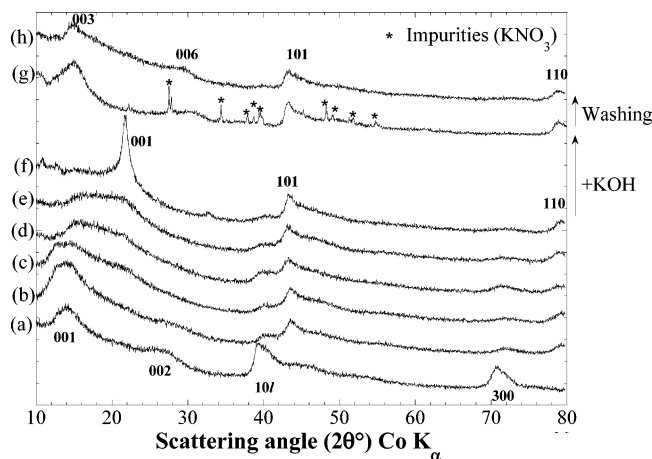


**Figure 5.** X-ray diffraction patterns of samples taken off during the two-step ozonation of  $\alpha$ II-Ni(OH)<sub>2</sub>: (a) initial  $\alpha$ II-Ni(OH)<sub>2</sub> phase; (b) after 10 min under a moist ozone atmosphere; (c) after 20 min; (d) after 30 min; (e) after 40 min; (f) after 6 h; (g) after 8 h under a moist ozone atmosphere with KOH; (h) sample g washed.

As the reaction progresses, the  $\beta$ II-Ni(OH)<sub>2</sub> phase gradually disappears, leaving only  $\beta$ III-NiOOH and  $\gamma$ III-NiOOH phases. It is only after a second KOH addition that the reaction is complete, yielding a pure  $\gamma$ III-NiOOH phase as the final product (Figure 4f) for which the oxidation degree of nickel was found to be  $3.50 (\pm 0.05)$ . A TEM study done on an intermediate sample did confirm the pseudomorphous and topotactic character of the reaction.

**Ozonation of the  $\alpha$ II-Ni(OH)<sub>2</sub> Hydroxide.** *Description of the Starting Material.* The  $\alpha$ II-Ni(OH)<sub>2</sub> phase has also a brucite-type structure, but with turbostratic disorder, the NiO<sub>2</sub> layers being randomly oriented along the *c* axis. Its diffraction pattern (Figure 5a or 9a) is poor, and presents only asymmetric bands. This phase crystallizes in the hexagonal system with the  $P\bar{3}m1$  space group, and contains water, carbonates, and nitrates in the interlayer space, the cell parameters being  $a = 5.34 \text{ \AA}$  and  $c = 7.60 \text{ \AA}$ .<sup>15</sup> From a morphological point of view,  $\alpha$ II-Ni(OH)<sub>2</sub> appears as aggregates of very thin tangled fibers without any particular morphology (Figure 9 d).<sup>14,15</sup> SAED on such aggregates (not shown here) allows the observation of diffraction rings

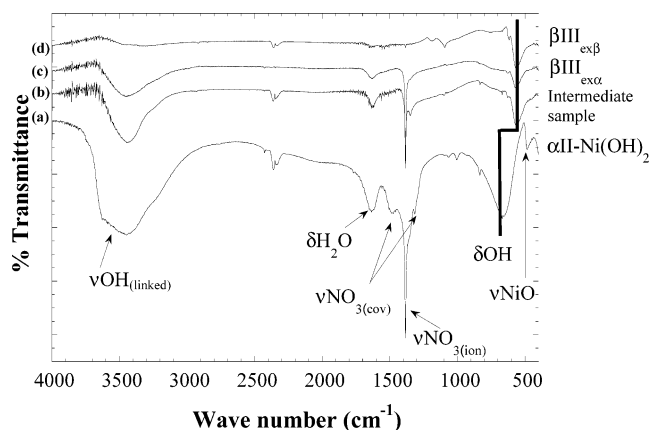


**Figure 6.** FT-IR spectra of (a) initial  $\alpha$ II-Ni(OH)<sub>2</sub>, (b) a sample after 0.5 h under moist ozone, (c)  $\beta$ III<sub>exα</sub>, and (d)  $\beta$ III<sub>exβ</sub>.

directly corresponding to the asymmetric lines appearing on the XRD patterns.

**Protocol 1.** The same experimental protocol used for  $\beta$ II-Ni(OH)<sub>2</sub> was applied to  $\alpha$ II-Ni(OH)<sub>2</sub>, that is to say that the pure  $\alpha$ II-Ni(OH)<sub>2</sub> phase was treated under moist ozone, and the treatment was continued after KOH addition. Several samples were taken off and characterized in the course of the oxidation. Figure 5 exhibits the diffraction patterns of these samples. It clearly appears that a transformation of  $\alpha$ II-Ni(OH)<sub>2</sub> into  $\beta$ III-NiOOH occurs during the first 6 h of ozonation. The nickel oxidation degree within the  $\beta$ III-NiOOH phase formed after 6 h was estimated by iodometric titration to be  $2.95 (\pm 0.05)$ , a value usually found for  $\beta$ III-NiOOH issued from  $\beta$ II-Ni(OH)<sub>2</sub>. A range of samples removed every 10 min from the beginning of the reaction helped to follow the phase composition evolution (Figure 5a–e). Note that the broad and asymmetric bands characteristic of  $\alpha$ II-Ni(OH)<sub>2</sub> slowly disappear, while new reflections grow around  $22^\circ$ . The obtained final phase (Figure 5f) presents cell parameters  $a = 2.42 \text{ \AA}$  and  $c = 4.81 \text{ \AA}$  very close to those of a typical  $\beta$ III-NiOOH (namely,  $a = 2.41 \text{ \AA}$  and  $c = 4.83 \text{ \AA}$ ). Nevertheless, the diffraction lines of this  $\beta$ III-NiOOH phase are asymmetric as in the case of the parent turbostratic structure. This observation led us to perform a more thorough characterization using FT-IR, TGA, and HRTEM of the structure, and the morphology of this phase is termed from now on “ $\beta$ III<sub>exα</sub>” in opposition to “ $\beta$ III<sub>exβ</sub>”, which corresponds to the pure  $\beta$ III-NiOOH oxyhydroxide issued from the treatment of  $\beta$ II-Ni(OH)<sub>2</sub> by ozone.

In Figure 6, we report the FT-IR spectra of the initial  $\alpha$ II-Ni(OH)<sub>2</sub> (Figure 6a), a sample treated for 30 min under moist ozone (Figure 6b),  $\beta$ III<sub>exα</sub> (Figure 6c), and  $\beta$ III<sub>exβ</sub> (Figure 6d).  $\alpha$ II-Ni(OH)<sub>2</sub> presents the typical infrared vibrations of a turbostratic phase: the water is responsible for both the large band around  $3600 \text{ cm}^{-1}$  ( $\nu_{\text{OH-linked}}$ ) and the band at  $1635 \text{ cm}^{-1}$  ( $\delta_{\text{H}_2\text{O}}$ ), while hydroxyls contained in the sheets are characterized by the band appearing at  $660 \text{ cm}^{-1}$  ( $\delta_{\text{OH}}$ ). Two types of nitrates are present: covalent nitrates ( $\nu_{\text{NO}_3}$  at  $1485$ ,  $1314$ , and  $1005 \text{ cm}^{-1}$ ) and ionic nitrates ( $\nu_{\text{NO}_3}$  at  $1383 \text{ cm}^{-1}$ ). The band corresponding to the Ni–O bond vibration appears at  $484 \text{ cm}^{-1}$ . As compared to that of the fresh sample, the IR spectrum of the sample removed after 30 min of

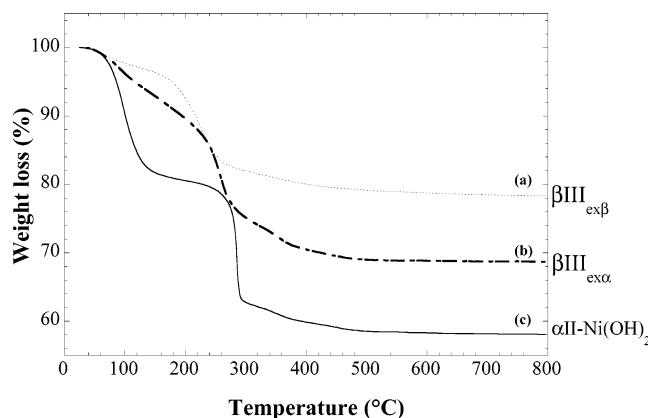


Figure 7. TGA curves of (a)  $\beta\text{III}_{\text{ex}\beta}$ , (b)  $\beta\text{III}_{\text{ex}\alpha}$ , and (c)  $\alpha\text{II-Ni(OH)}_2$ .

ozonation presents a few differences. The  $\delta_{\text{OH}}$  band has shifted from 660 to 560  $\text{cm}^{-1}$ , indicating a transformation from the reduced  $\text{Ni(OH)}_2$  phase to the oxidized  $\text{NiOOH}$ .<sup>18</sup> At the same time, the broad band around 3600  $\text{cm}^{-1}$  ( $\nu_{\text{OH-linked}}$ ) and the band at 1635  $\text{cm}^{-1}$  ( $\delta_{\text{H}_2\text{O}}$ ) become smaller, while most of the covalent nitrates have disappeared in contrast with ionic nitrates that are still present.<sup>19</sup> Finally, in the  $\beta\text{III}_{\text{ex}\alpha}$  spectrum,  $\delta_{\text{OH}}$  remains at 560  $\text{cm}^{-1}$ , indicating that the phase is in an oxidized state, and the covalent nitrates have completely disappeared. Thus, the difference between  $\beta\text{III}_{\text{ex}\alpha}$  and  $\beta\text{III}_{\text{ex}\beta}$  lies mostly in the presence of ionic nitrates within the  $\beta\text{III}_{\text{ex}\alpha}$  phase.

TGA measurements, carried out on the same products (i.e.,  $\alpha\text{II-Ni(OH)}_2$ ,  $\beta\text{III}_{\text{ex}\alpha}$ , and  $\beta\text{III}_{\text{ex}\beta}$ ), support this result (Figure 7). During the heating of  $\beta\text{III}_{\text{ex}\alpha}$ , three phenomena are observed. Around 91 °C, a small amount of water is lost. At 228 °C, a weight loss due to the deshydroxylation of  $\text{NiOOH}$  into  $\text{NiO}$  occurs. Finally, at 350 °C, a third weight loss takes place that, according to the literature,<sup>20,21</sup> can be attributed to the loss of nitrates. This latter weight loss does not appear for  $\beta\text{III}_{\text{ex}\beta}$ . Thus, combined infrared and thermogravimetric results confirm the presence of ionic nitrates within the  $\beta\text{III}_{\text{ex}\alpha}$  phase, as opposed to the  $\beta\text{III}_{\text{ex}\beta}$  phase. Finally, the amount of nitrates was also chemically analyzed: for  $\beta\text{III}_{\text{ex}\alpha}$ , the ratio  $\text{NO}_3/\text{Ni}$  is equal to 0.20 in contrast to the measured ratio of 0.00 for  $\beta\text{III}_{\text{ex}\beta}$ . Finally, the presence of water within the  $\beta\text{III}_{\text{ex}\alpha}$  phase highlighted by both the infrared and TGA techniques and should be due to adsorbed water. The  $\beta\text{III}_{\text{ex}\alpha}$  phase is supposed to adsorb more water than the  $\beta\text{III}_{\text{ex}\beta}$  phase since the surface of the former is bigger.

The characterization of  $\beta\text{III}_{\text{ex}\alpha}$  was completed by HRTEM studies. Its morphology is very close to that of  $\alpha\text{II-Ni(OH)}_2$  starting material: the sample consists of aggregates of very thin tangled films without any particular morphology. Using high resolution, it appears that the  $\beta\text{III}_{\text{ex}\alpha}$  aggregates are composed of sheets with 4.8 Å interlamellar distances (see Figure 8). The similar morphologies between the parent  $\alpha\text{II-Ni(OH)}_2$

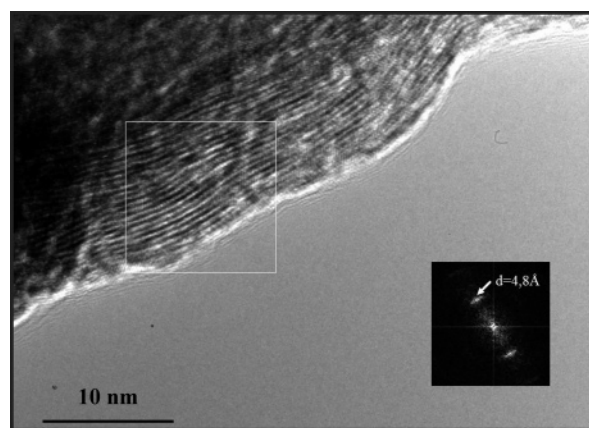


Figure 8. HRTEM photo and associated FFT (fast Fourier transform) performed on the  $\beta\text{III}_{\text{ex}\alpha}$  phase.

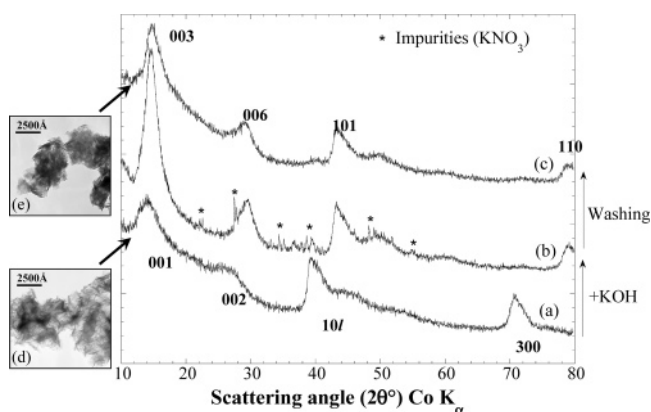


Figure 9. X-ray diffraction patterns of samples taken off during the one-step ozonation of  $\alpha\text{II-Ni(OH)}_2$ : (a) initial  $\alpha\text{II-Ni(OH)}_2$  phase; (b) after 8 h under a moist ozone atmosphere with KOH; (c) sample b washed. Corresponding scanning electron microscopy pictures of the initial  $\alpha\text{II-Ni(OH)}_2$  phase (d) and of the final  $\gamma\text{III-NiOOH}$  phase resulting from the one-step ozonation process (e).

$\text{Ni(OH)}_2$  and the new  $\beta\text{III}_{\text{ex}\alpha}$  phase prepared by ozonation prove that the reaction takes place in the solid state.

If potassium hydroxide is added to  $\beta\text{III}_{\text{ex}\alpha}$  and the ozonation is pursued, we observe the formation of  $\gamma\text{III-NiOOH}$  oxyhydroxide. It is important to note the appearance at the same time of  $\text{KNO}_3$  impurities that can easily be removed by washing, as proved by XRD patterns (Figure 5g,h). The resulting  $\gamma\text{III-NiOOH}$  phase is poorly crystallized as indicated by the broad peaks present in its XRD pattern. Moreover, its oxidation degree reaches 3.55 ( $\pm 0.05$ ).

**Protocol 2.** Samples were also taken in the course of oxidation of the  $\alpha\text{II-Ni(OH)}_2/\text{KOH}$  mixture, and studied by XRD and TEM. The results are presented in Figure 9. A transformation from  $\alpha\text{II-Ni(OH)}_2$  into  $\gamma\text{III-NiOOH}$  occurs directly, and rapidly and a gradual change of cell parameters is observed with conservation of the asymmetry of the peaks. This is indicative of a turbostratic structure for the  $\gamma\text{III-NiOOH}$  phase as for the initial  $\alpha\text{II-Ni(OH)}_2$  phase. As already described in the previous two-step oxidation process,  $\text{KNO}_3$  formed during the reaction can be removed by washing with water. The TEM pictures (Figure 9d,e) taken of both initial and final products revealed no morphological changes. The  $\gamma\text{III-NiOOH}$  phase obtained by ozonation of  $\alpha\text{II-Ni(OH)}_2$  hydroxide is constituted by aggregates of the

- (18) Kober, F. P. *J. Electrochem. Soc.* **1967**, *114*, 3, 215–218.  
 (19) Portemer, F. Thèse de doctorat d'état, Université de Picardie Jules Verne, Amiens, 1997.  
 (20) Fievet, F.; Germi, P.; De Bergerin, F.; Figlarz, M. *J. Appl. Crystallogr.* **1979**, *12*, 387.  
 (21) Genin, P.; Delahaye-Vidal, A.; Portemer, F.; Tekaiia-Elhsissen, K.; Figlarz, M. *Eur. J. Solid State Inorg. Chem.* **1991**, *28*, 505–518.

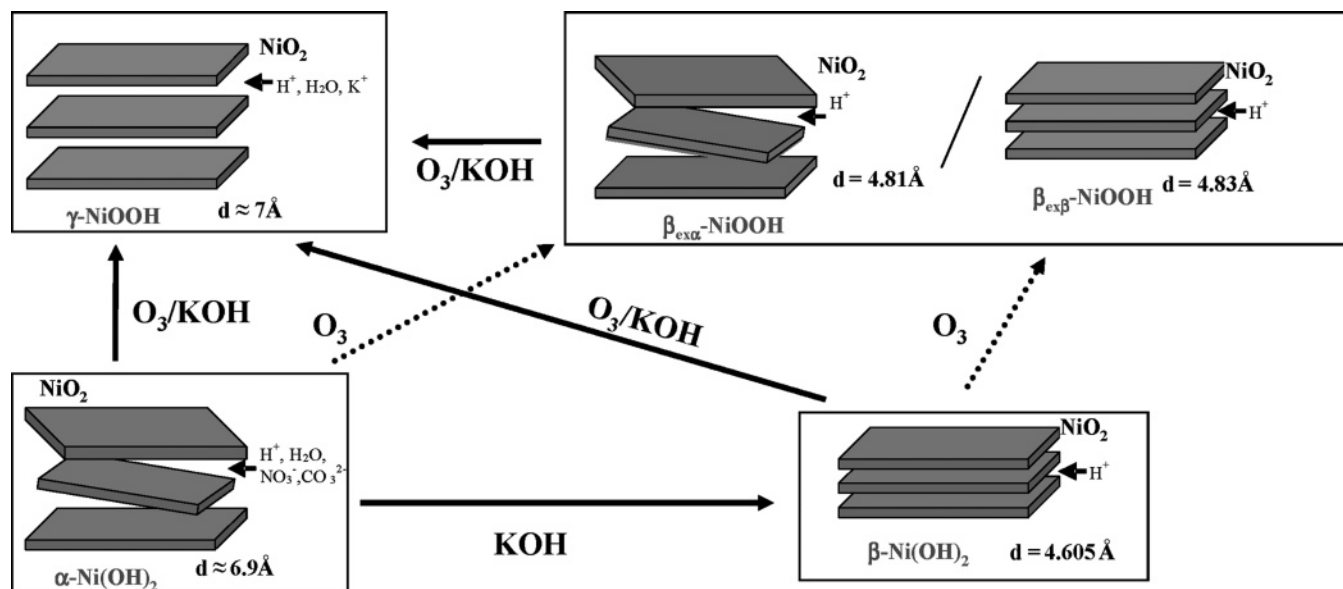


**Figure 10.** Modification of the Bode diagram<sup>6</sup> to include the “new”  $\beta_{III\text{ex}\alpha}$  phase obtained by ozonation of  $\alpha\text{II-Ni(OH)}_2$ . The resulting diagram and the relationships between the phases involved can be compared with those observed in our previous study on cobalt hydroxides.<sup>13</sup>

same type as the starting material. The oxidation degree for this  $\gamma_{III}\text{-NiOOH}$  phase is about  $3.55 (\pm 0.05)$ , similar to the value measured on the  $\gamma_{III}\text{-NiOOH}$  phase resulting from the two-step reaction.

### Discussion

The above results have shown that the chemical oxidation of  $\text{Ni(OH)}_2$  by ozone proceeds through different reaction paths depending on the nature of the starting phase. Independently of the addition of alkaline ions, it is clear that the ozonation of  $\beta_{II}\text{-Ni(OH)}_2$  is a topotactic and pseudomorphous reaction taking place in the solid state in total agreement with previous reports.<sup>22,23</sup> However, the real advantage of the ozonation lies in the fact that the phases formed are better controlled. Obtaining pure  $\beta_{III}\text{-NiOOH}$  turns out to be very simple by just ozonating without the presence of alkaline ions. On the other hand, the addition of cations such as  $\text{Na}^+$  or  $\text{K}^+$  in the right proportion during oxidation leads to the formation of pure  $\gamma_{III}\text{-NiOOH}$ . It is worth noting that when the reaction takes place in aqueous media, the presence of alkaline ions is impossible to avoid; thus,  $\beta_{III}\text{-NiOOH}$  prepared by solution often presents impurities of  $\gamma_{III}\text{-NiOOH}$ . In other terms, ozonation turns out to be an easier way to synthesize single-phase  $\beta_{III}\text{-NiOOH}$ .

With regard to the  $\alpha_{II}\text{-Ni(OH)}_2$  hydroxide, the following experimental observations done during ozonation made us conclude that (i) the formation of a  $\beta_{III\text{ex}\alpha}$  phase containing ionic nitrates and water molecules, (ii) the obtaining of amorphous  $\gamma_{III}$  after the ozonation of  $\beta_{III\text{ex}\alpha}$  with potassium hydroxide, and (iii) the appearance of  $\text{KNO}_3$  impurities upon  $\text{KOH}$  addition. These facts led us to propose an oxidation mechanism that is different from the one taking place in aqueous solution. We believe that the first step in the oxidation of  $\alpha_{II}\text{-Ni(OH)}_2$  by ozone is the oxidation of Ni-

(II) to Ni(III) with concomitant proton expulsion, as commonly observed upon nickel hydroxide oxidation in aqueous media. Nevertheless, the infrared study proves that the  $\beta_{III\text{ex}\alpha}$  phase, prepared without the presence of alkaline cations, no longer contains covalent nitrates (initially present in the  $\alpha$  phase within the interlamellar space), and that the  $\nu_{\text{OH}}$  band intensity has drastically decreased. These observations imply that, upon ozonation, the interlayer water molecules contained in  $\alpha_{II}\text{-Ni(OH)}_2$  must be expelled from the structure together with the covalently bonded nitrates to yield the  $\beta_{III\text{ex}\alpha}$  phase. The expulsion of these species, playing the role of pillars within the  $\alpha$  phase, causes the structure to collapse and the interlayer distance to decrease from 6.9 to 4.8 Å to finally form  $\beta_{III\text{ex}\alpha}$  that, as proved by the IR study, still contains ionic nitrates on the surface layers. As soon as potassium hydroxide is added to the  $\beta_{III\text{ex}\alpha}$  phase under the ozone flow, not only do these ionic nitrates combine with  $\text{K}^+$  cations to form the  $\text{KNO}_3$  impurities as detected by X-ray diffraction, but also the  $\beta_{III\text{ex}\alpha}$  phase transforms into  $\gamma_{III\text{ex}\beta}$  with concomitant potassium ion insertion consistent with the observed increase in the interlayer distance from 4.8 to 7 Å. Concerning the one-step reaction (protocol 2), it could be considered that the potassium ions directly replace the water molecules and nitrate ions as pillars in the pristine  $\alpha_{II}$  phase, so that the interlayer distance remains almost the same, with the overall process being similar to that taking place in aqueous media.<sup>22</sup> In this case, because the mechanism does not involve an intermediate phase with a reduced interlayer distance, one should expect a preservation of the material crystallinity as confirmed by the X-ray diffraction patterns of the  $\gamma_{III}\text{-NiOOH}$  phase that present well-defined Bragg peaks as for the starting phase.

In light of the above observations, we could propose a slight modification of the Bode diagram<sup>6</sup> (which initially describes the redox and structural relationships among the four main phases reported:  $\alpha_{II}$ ,  $\beta_{II}$ ,  $\beta_{III}$  (here denoted  $\beta_{III\text{ex}\beta}$ ), and  $\gamma_{III}$  in aqueous media) to include the newly prepared  $\beta_{III\text{ex}\alpha}$  phase (see Figure 10). It is generally agreed

(22) Delahaye-Vidal, A. Thèse de doctorat d'état, Université de Picardie Jules Verne, Amiens, 1986.

(23) Delahaye-Vidal, A.; Beaudoin, B.; Sac-Epée, N.; Tekaiia-Elhissen, K.; Audemer, A.; Figlarz, M. *Solid State Ionics* **1996**, *84*, 234–238.

that the storage of  $\alpha$ II-type hydroxide in an alkaline medium allows the formation of a  $\beta$ II-type phase by a dissolution/recrystallization process. Besides, numerous studies performed in aqueous media report the preparation of  $\beta$ III by moderate oxidation of  $\beta$ II, whereas  $\gamma$ III oxyhydroxide is produced after overoxidation of  $\beta$ II, either inside a battery or in a NaClO/KOH solution.<sup>9,10</sup> According to our results, using a “dry” oxidation process, another  $\beta$ III<sub>ex $\alpha$</sub>  phase can be isolated in the oxidation of  $\alpha$ II and therefore should be added to this diagram. The main differences between the  $\beta$ III phases are only morphological as in both cases oxidation takes place in the solid state, and the final phase retains the characteristics of the reduced precursor phase. However, despite the importance of these fundamental findings, it should be stressed that, in real battery operating conditions, the chances of promoting the formation of  $\beta$ III<sub>ex $\alpha$</sub>  are slim, owing to the presence of alkaline cations in the electrolyte solution.

### Conclusion

This study presents in detail the behavior of both  $\alpha$ II and  $\beta$ II nickel hydroxides upon ozonation. We demonstrate that

the ozone allows the formation of pure either  $\beta$ III and  $\gamma$ III nickel oxyhydroxides, depending on the presence or absence of alkaline ions. Regarding ozonation of the  $\beta$ II-Ni(OH)<sub>2</sub> phase, the reaction mechanisms were found to be similar to those taking place during oxidation in aqueous media. The most important result of this study concerns the synthesis of a new phase noted  $\beta$ III<sub>ex $\alpha$</sub>  isolated during the two-step ozonation of  $\alpha$ II-Ni(OH)<sub>2</sub>. Compared with a  $\beta$ III oxyhydroxide issued from the ozonation of the  $\beta$ II phase ( $\beta$ III<sub>ex $\beta$</sub> ), the  $\beta$ III<sub>ex $\alpha$</sub>  phase presents a few differences listed as follows: (i) (002) and (101) diffraction peaks are abnormally asymmetric, (ii) it contains ionic nitrates, and (iii) it is composed of agglomerates of particles with no specific morphology as the  $\alpha$  phase precursor used to prepare it. In addition to the specific results obtained on the nickel system, this study highlights, once more, the interest of developing a dry oxidation method.

**Acknowledgment.** We are largely indebted to L. Dupont for HRTEM pictures and to A. Delahaye-Vidal for helpful discussions. We also thank the Gillette Co. for financial support.

CM040133+